
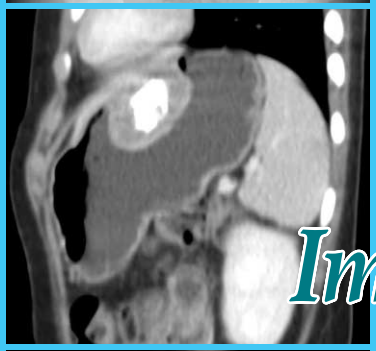
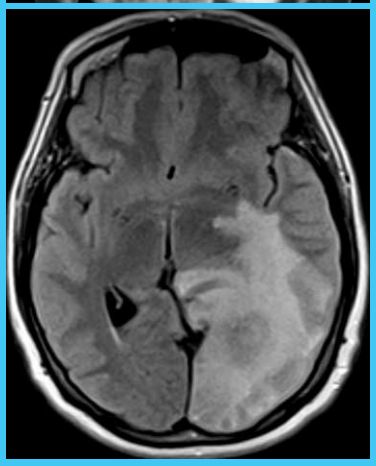

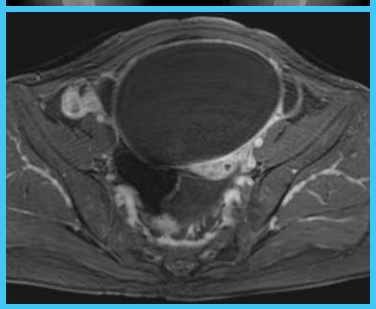


# KCR 2012

# *Answers for Image Interpretation Session*

**October 18 (Thu), 14:00 - 15:30**
**Grand Ballroom 101 - 105, Convention Hall 1F, Coex**

- Moderator — **Hyo-Keun Lim**
  *Samsung Medical Center*
- Discussers
  **AB Hun Kyu Ryeom**
  *Kyungpook National University Hospital*
  **CH Hwan Seok Yong**
  *Korea University Guro Hospital*
  **GU Hak Jong Lee**
  *Seoul National University Bundang Hospital*
  **NR Dae Seob Choi**
  *Gyeongsang National University Hospital*
  **PD Choon Sik Yoon**
  *Gangnam Severance Hospital*

대한영상의학회
The Korean Society of Radiology


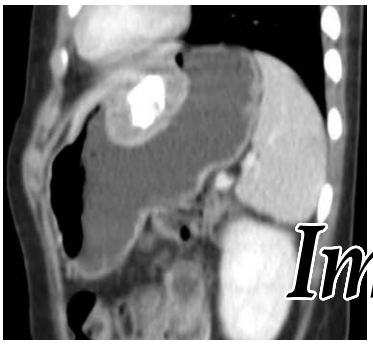
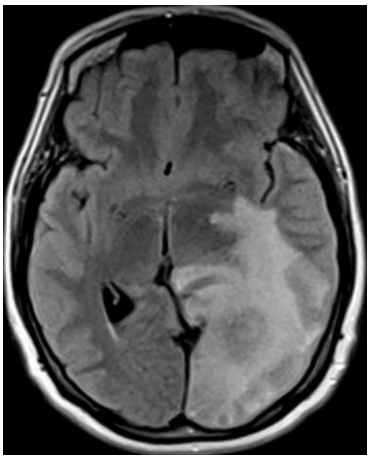

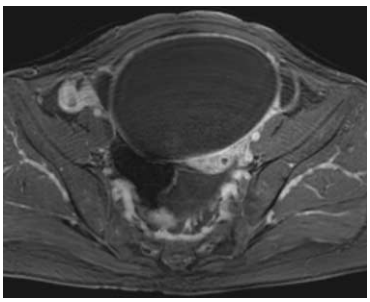


# KCR 2012

# *Answers for Image Interpretation Session*

**October 18 (Thu), 14:00 - 15:30**
**Grand Ballroom 101 - 105, Convention Hall 1F, Coex**

- Moderator **Hyo-Keun Lim**
  *Samsung Medical Center*
- Discussers **AB Hun Kyu Ryeom**
  *Kyungpook National University Hospital*
  **CH Hwan Seok Yong**
  *Korea University Guro Hospital*
  **GU Hak Jong Lee**
  *Seoul National University Bundang Hospital*
  **NR Dae Seob Choi**
  *Gyeongsang National University Hospital*
  **PD Choon Sik Yoon**
  *Gangnam Severance Hospital*

대한영상의학회
The Korean Society of Radiology

# Image Interpretation Session

## Case 1: Pediatric


| | |
|---|---|
| **Discusser** | Choon-Sik Yoon |
| **Country** | Republic of Korea |
| **Current Affiliation** | Gangnam Severance Hospital |


| | |
|---|---|
| **Age/Gender** | 5/F |
| **Chief complaint** | Epigastric pain (10 months) |

A

B

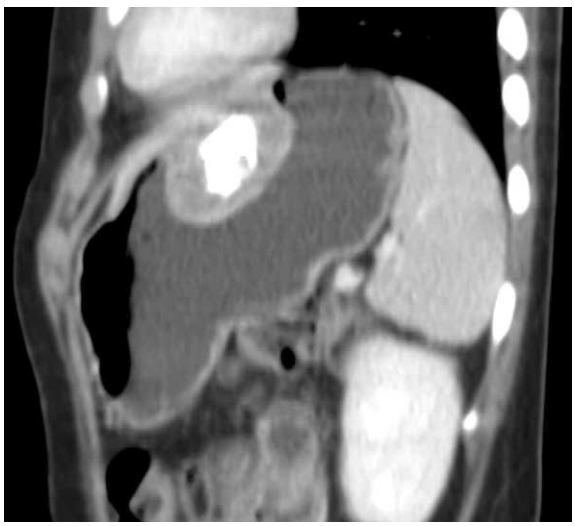

C

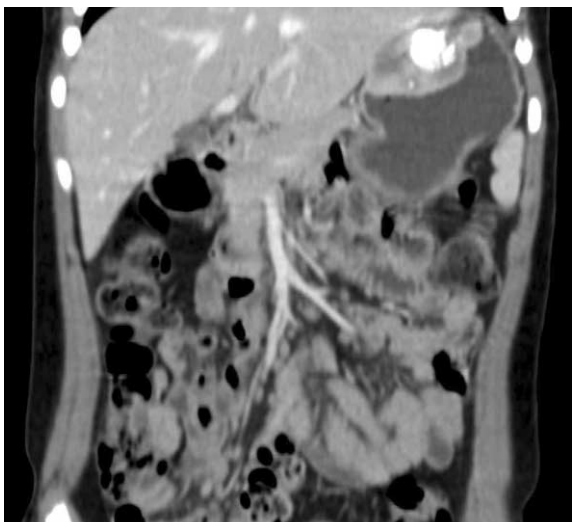

D

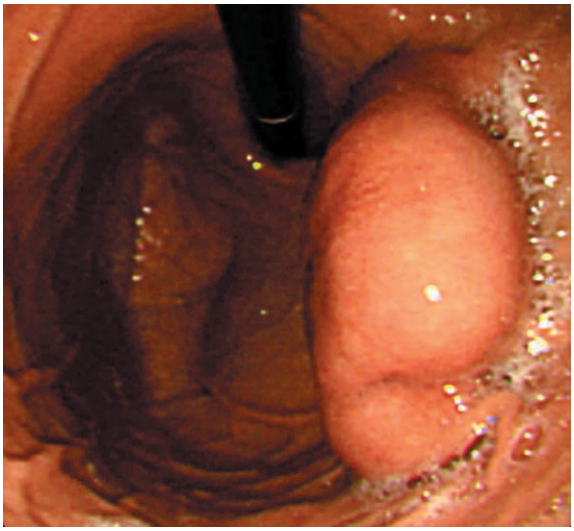

E

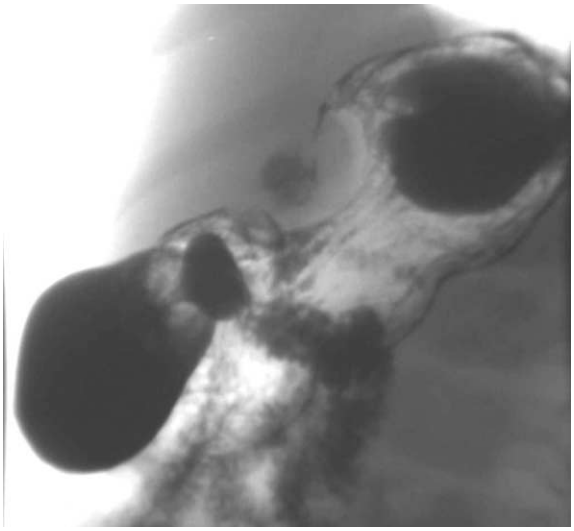

F

## Case 1

### History

A 5-year-old girl presented with epigastric pain for 10 months. Laboratory findings were within normal range.

### Findings

Plain radiograph of the abdomen shows abnormal amorphous calcification in the left upper abdomen.

Contrast-enhanced abdominal CT scan demonstrates a well-defined, lobulated mass with heterogeneous enhancement in the gastric high body. The mass shows dense calcification and endoluminal growth pattern.

An oblique view obtained after barium swallowing shows a smoothly marginated filling defect containing calcification, that forms obtuse angles with the gastric wall suggesting a submucosal mass. Ulceration was not demonstrated.

Endoscopic examination of the stomach reveals a polypoid mass covered by normal-appearing mucosa at the anterior wall of gastric high body.

### Differential Diagnosis

GIST
Hamartoma
Teratoma
Carcinoid tumor

### Diagnosis: *Gastric inflammatory myofibroblastic tumor*

### Discussion

Gastric inflammatory myofibroblastic tumors (IMT) are rare benign lesions that most often affect young adults and children. The tumor predominantly affects females (ratio, 4:1) between the ages of 4 months and 15 years (mean age, 7 years). IMT is a benign solid tumor composed mainly of spindle-shaped cells and has a chronic inflammatory component consisting of plasma cells, lymphocytes, and occasionally histiocytes. This lesion may not be differentiated from malignant tumors radiologically because of its local invasiveness and the tendency to recur. Additionally, some reported the malignant transformation of IMT and lymphoreticular malignancy arising in the residual IMT.

The clinical presentation of an IMT can vary and depends on the site of origin. Symptoms include weight loss, fever, and a general constellation of inflammatory biomarkers such as anemia, thrombocytosis, elevated ESR, and hypergammaglobulinemia. The clinical and laboratory abnormalities typically resolve after surgical resection but can be associated with local recurrence of the tumor. The radiologic findings of intraabdominal IMT are nonspecific. It may show solid, sometimes heterogeneous, well-demarcated (or multilobulated) spherical mass. They may show infiltrative feature of the IMT as occurred in some cases.

The current treatment for a gastric IMT is complete surgical resection, with chemotherapy playing a role before surgery if complete excision is not possible.

### References

1. Kamak I, Senocak ME, Ciffci AO, Caqlar M, Binqol-Kologlu M, Tanyel FC, et al. Inflammatory myofibroblastic tumor in children: diagnosis and treatment. J Pediatr Surg 2001;36:908-12
2. Kim KA, Park CM, Lee JH, Cha SH, Park SW, Hong SJ, et al. Inflammatory myofibroblastic tumor of the stomach with peritoneal dissemination in a young adult: imaging findings. Abdom Imaging 2004;29:9-11
3. Al Hatlani M, Ratcliffe EM. Endoscopic visualization of a gastric polypoid mass: a rare pediatric presentation of an inflammatory myofibroblastic tumor. Gastrointest Endosc. 2010;72:894-5

# Case 2: Neuro


| | |
|---|---|
| Discusser | Dae Seob Choi |
| Country | Republic of Korea |
| Current Affiliation | Gyeongsang National University Hospital |


| | |
|---|---|
| Age/Gender | 57/F |
| Chief complaint | Headace (onset: a month ago) |

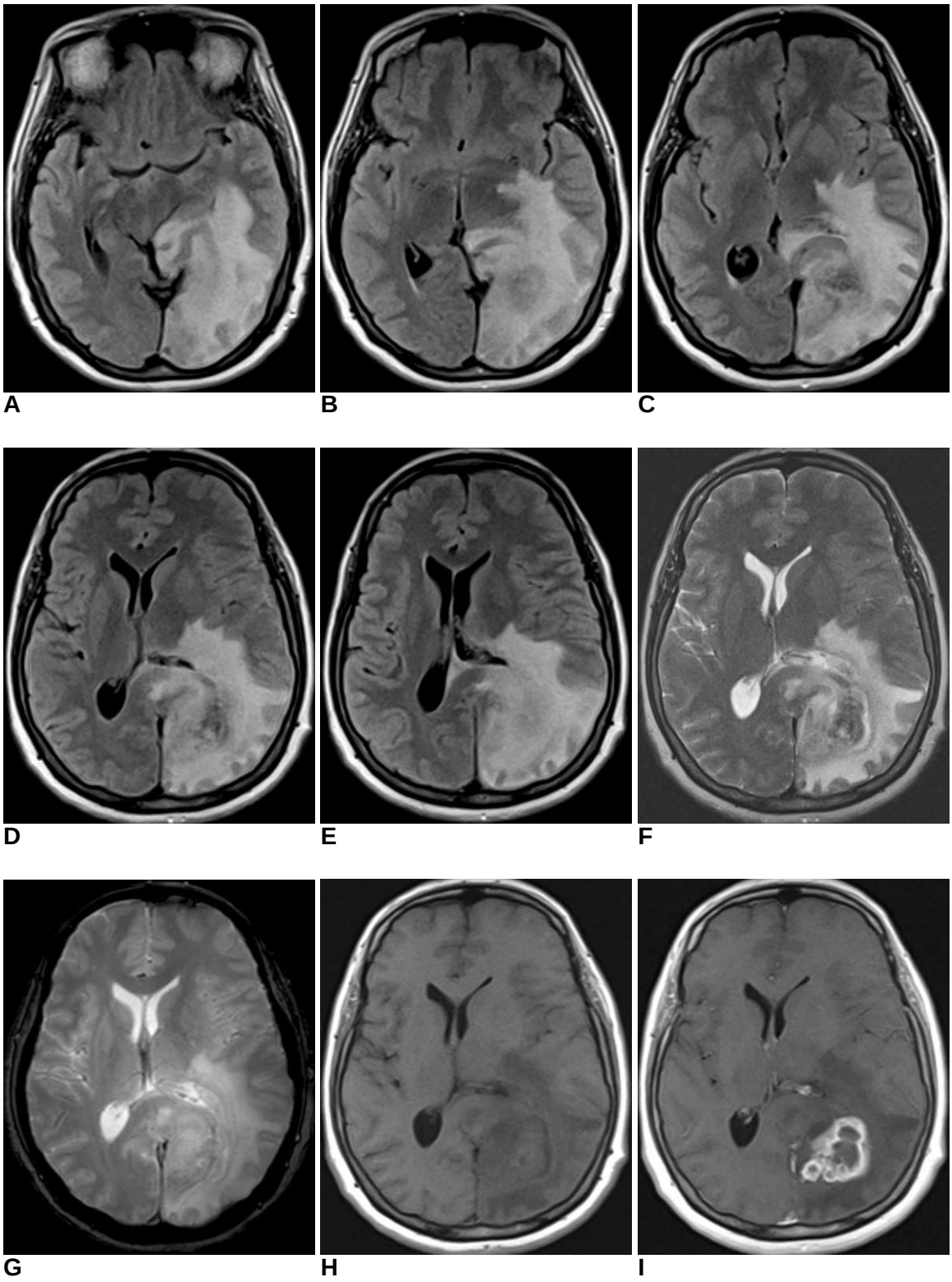

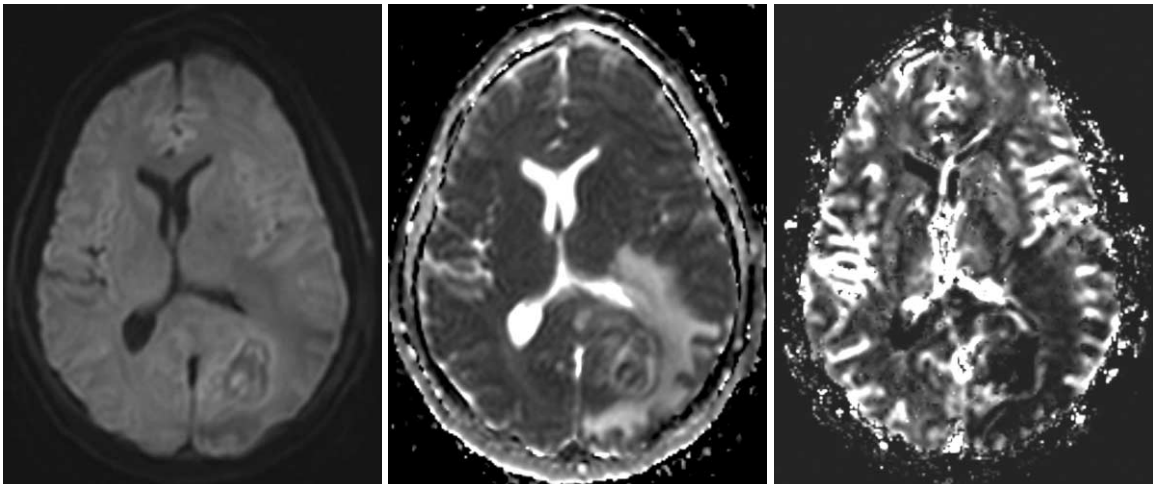

**J** **K** **L**

## Case 2

### History

A 56-year-old female presented with headache and dizziness for a month. Recently, a right hemianopsia was accompanied.

### Findings

Axial T2 FLAIR images show slightly hyperintense mass with severe perilesional edema in the left occipital lobe. The mass shows well-defined margin and mixed signal intensity with heterogeneous iso- or hypointense wall on T2WI, which shows no calcification nor hemorrhage on gradient echo image. T1WI shows central mixed iso- and hyperintense portion and hyperintense rim. After contrast material injection, smooth ring enhancement is seen. DWI shows restricted diffusion in the center. The capsule shows no contrast enhancement on rCBV map compatible with the hypoperfusion (hypovascularization).

### Differential Diagnosis

Pyogenic abscess
Metastasis
Tuberculoma

### Diagnosis: *Tuberculoma*

### Discussion

Involvement of the CNS is seen in approximately 5% of patients with tuberculosis. CNS tuberculosis usually results from hematogenous spread. However, it may result from direct rupture or extension of a subependymal or subpial focus (Rich focus) and may be located in the meninges, brain, or spinal cord. CNS tuberculosis can manifest in a variety of forms, including tuberculous meningitis, tuberculomas, tuberculous abscesses, tuberculous cerebritis, and miliary tuberculosis.

The most common CNS parenchymal lesion of tuberculosis is tuberculoma (tuberculous granuloma). This lesion may be solitary, multiple, or miliary and may be seen anywhere within the brain parenchyma, although it most commonly occurs within the frontal and parietal lobes.

The MRI findings depend on whether the tuberculoma is caseating, and if so, whether the center is liquid or solid. A noncaseating tuberculoma is hypointense relative to gray matter on T1WI and hyperintense on T2WI, with homogeneous gadolinium enhancement. Caseating tuberculomas with a solid center are iso- to hypointense on both T1- and T2WI. They usually have a variable amount of surrounding edema, which is hyperintense on T2WI. Caseating tuberculomas with a liquid center are hypointense on T1WI and centrally hyperintense on T2WI, with a peripheral hypointense rim on T2WI representing the capsule.

Histologic correlation revealed that the central iso- or hyperintensity on T1WI corresponded to caseation necrosis with adjacent inflammatory infiltrates. Surrounding slight hyperintense and hypointense rims corresponded to a layer of collagenous fibrosis and a layer of outer inflammatory infiltrates, respectively. The variable signal intensity of central caseation necrosis might be related to the variable protein concentration which has varied T1 relaxation time. Rim enhancement is usually seen at gadolinium-enhanced MRI. The core of the lesion showed restricted diffusion similar to pyogenic abscess. However, the ADC values were much lower than necrotic neoplastic lesions, because of the high viscousity in the caseation necrosis resulting from the presence of intact inflammatory cells. The low rCBV on perfusion-weighted image is attributed to the high amounts of mature collagen and decreased neovascularity. The rCBV ratios in the capsular portions of brain abscesses were significantly lower than those of malignant tumors compared with normal white matter.

### References

1. Burrill J, Williams CJ, Bain G, Conder G, Hine AL, Misra RR. Tuberculosis: a radiologic review. Radiographics 2007;27:1255-1273
2. Kim TK, Chang KH, Kim CJ, Goo JM, Kook MC, Han MH. Intracranial tuberculoma: comparison of MR with pathologic findings. AJNR Am J Neuroradiol 1995;16:1903-1908
3. Castillo M, Mukherji SK. Diffusion-weighted imaging in the evaluation of intracranial lesions. Semin Ultrasound CT MR 2000;21:405-416
4. Holmes TM, Petrella JR, Provenzale JM. Distinction between cerebral abscesses and high-grade neoplasms by dynamic susceptibility contrast perfusion MRI. AJR Am J Roentgenol 2004;183:1247-1252
5. Erdogan C, Hakyemez B, Yildirim N, Parlak M. Brain abscess and cystic brain tumor: discrimination with dynamic susceptibility contrast perfusion-weighted MRI. J Comput Assist Tomogr 2005;29:663-667

# *Case 3: Chest*


| | |
|---|---|
| **Discusser** | Hwan Seok Yong |
| **Country** | Republic of Korea |
| **Current Affiliation** | Korea University Guro Hospital |


| | |
|---|---|
| **Age/Gender** | 16/M |
| **Chief complaint** | Chronic productive cough, mild dyspnea |

**A**

**B**

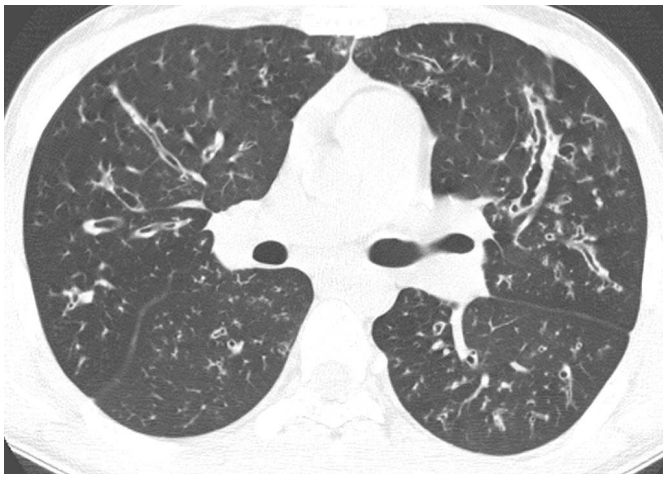

**C**

**D**

## Case 3

### History

A 16-year old male presented with chronic productive cough and mild dyspnea.

### Findings

Initial chest radiography revealed diffusely increased interstitial markings in both lungs.

High-resolution CT scan showed bilateral symmetric diffuse bronchiectasis and bronchiolitis with mucoid plugging in both lungs, which was more prominent in upper and mid-lung zones.

### Differential Diagnosis

Diseases that can manifest diffuse bronchiectasis and bronchiolitis include:

- Diffuse panbronchiolitis (DPB)
- Ciliary dyskinesia (immotile cilia syndrome)
- Allergic bronchopulmonary aspergillosis (ABPA)
- Non-tuberculous mycobacterial infection (NTM disease)
- Cystic fibrosis (CF)

### Lab. Findings

- Sweat chloride test (+)
- CFTR gene mutation (+)

### Pathologic Diagnosis

Explantation and transplantation of bilateral lungs was performed 8 years after the first visit. Pathologic examination of resected specimens showed:

1) diffuse bronchiolar dilatation with acute inflammation and luminal purulent material,
2) dense peribronchiolar fibrosis and honeycomb change.

### Diagnosis: *Cystic fibrosis*

### Discussion

Cystic fibrosis is one of most common inherited diseases in the Western world (autosomal recessive, 1/2,000–3,500 live births), but it is very rare in nonwhites (only 6 cases in Korea). It is known to be resulted from CFTR (CF transmembrane conductance regulator) gene mutation, which causes abnormal mucus formation in the airway, leading to luminal obstruction and recurrent bronchial inflammation and infection. Thus, the involved lungs show diffuse bronchiectasis, bronchiolitis and mucoid plugging. Although the major clinical manifestation of cystic fibrosis is an obstructive pulmonary disease (almost 100%) with recurrent bacterial respiratory infections, the incidence of pancreatic insufficiency (80–90%) is also highly reported. The diagnosis of cystic fibrosis is confirmed by a sweat chloride test (standard) ($\geq$ 60 mmol/L) and CFTR gene mutation ($\geq$ 2 among $\geq$ 1,500 types). The treatment includes antibiotics and anti-inflammatory agents for conservative purposes. Regarding the prognosis of cystic fibrosis, 80% of patients reach adulthood with a median survival $\geq$ 40 years.

HRCT findings include:

- Bronchiectasis (100%): bilateral symmetric, more severe in the upper lobes
- Bronchial wall thickening, mucus plugging
- Consolidation or atelectasis (80%)
- Cystic/bullous lesions: subpleural regions of upper lobes
- Branching centrilobular nodules (a tree-in-bud pattern) as an early sign of disease
- Air trapping on expiratory CT.

### References

1. Kim SJ, Lee M, Cha SI, et al. Standardized Sweat Chloride Analysis for the Diagnosis of Cystic Fibrosis in Korea. Korean J Lab Med 2008;28:274-281
2. Farrell PM, Rosenstein BJ, White TB, et al. Guidelines for diagnosis of cystic fibrosis in newborns through older adults: Cystic Fibrosis Foundation consensus report. J Pediatr 2008;153:S4-S14
3. Muller NL, Silva CIS. Specific causes of bronchiectasis. In: Imaging of the chest, Vol.2, Saunders, Philadelphia. 2008;1039-1055

# *Case 4: Gastrointestinal*



| | |
|---|---|
| **Discusser** | Hun Kyu Ryeom |
| **Country** | Republic of Korea |
| **Current Affiliation** | Kyungpook National University Hospital |



| | |
|---|---|
| **Age/Gender** | 70/M |
| **Chief complaint** | Intrahepatic mass on follow-up CT<br>(Hx. s/p Abdominoperineal resection for sigmoid colon cancer, 5 years ago) |

**A**

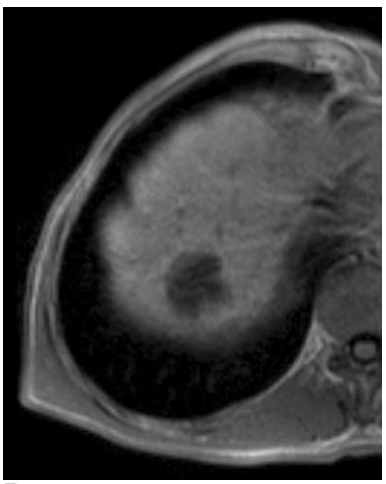

**B**

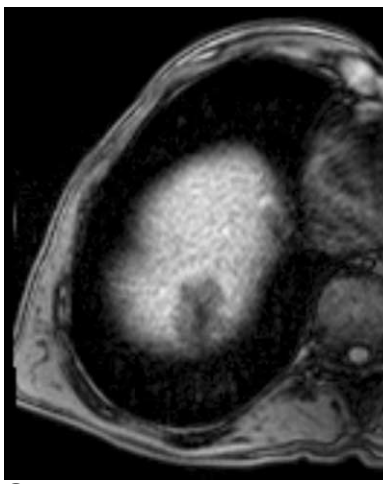

**C**

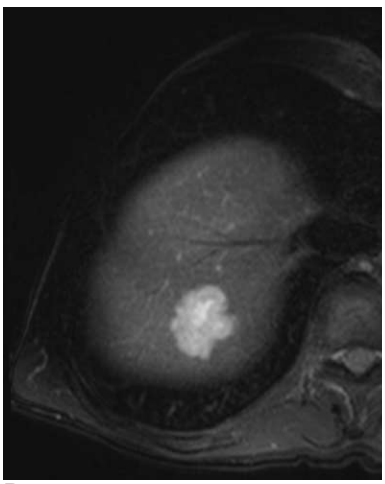

**D**

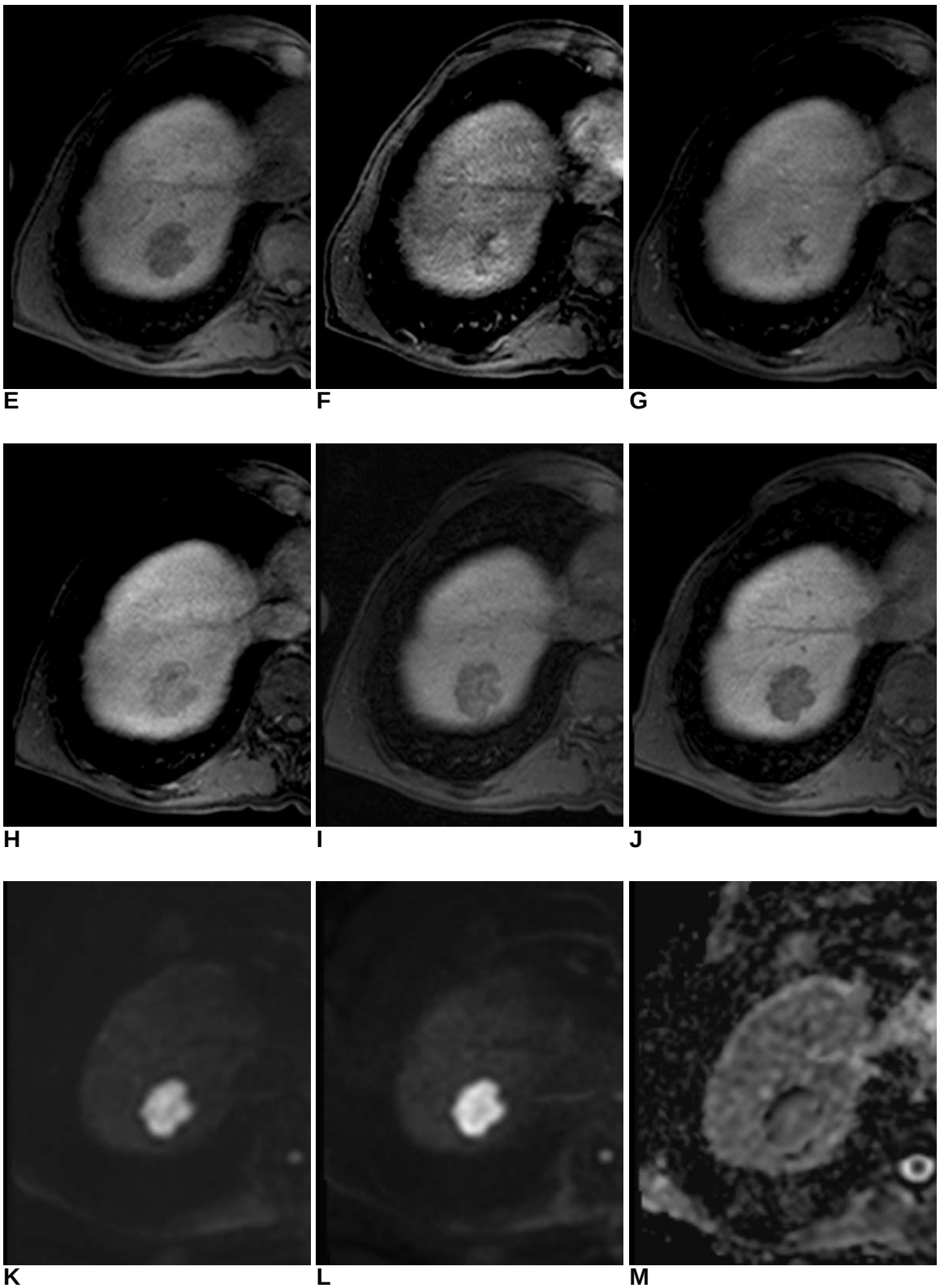
E
F
G
H
I
J
K
L
M

## Case 4

### History

A 70-year-old male presented with recently found abdominal mass on F/U CT who underwent abdominoperineal resection for sigmoid colon cancer 5 years ago.

### Findings

Recent abdominal CT reveals a 3.1 cm mass showing lobulating margin and heterogeneous enhancement with central low density portion surrounded by a low-density rim.

On MRI, the mass shows hypo intensity on T1WI, high signal intensity on T2WI, and defect on hepatobiliary phase. Gadoxetic acid-enhanced dynamic images show arterial hypervascularity and heterogeneous enhancement with washout portion on portal venous phase. Central scar showed hypointensity on T1WI, hyperintentensity on T2WI, and gradual enhancement.

### Differential Diagnosis

Metastasis from colon cancer
Cholangiocarcinoma
Scirrhous HCC
Combined hepatocellular and cholangiocarcinoma

### Diagnosis: *Scirrhous HCC with a central scar and scalloped margin*

### Discussion

According to WHO classification, scirrhous HCC is a subtype of HCC characterized by diffuse fibrosis along the sinusoid-like blood spaces and atrophy of tumor trabeculae. Radiological findings of scirrhous HCC include homogenous architecture, peripheral rim-like enhancement on arterial phase, followed by prolonged and delayed enhancement on equilibrium phase, absence of tumor capsule, and a retraction of the liver surface. Scirrhous HCC is often misdiagnosed as cholangiocarcinoma, metastasis, and combined hepatocellular and cholangiocarcinoma because of heterogenous enhancement in the arterial phase and prolonged enhancement in the late phase attributed to abundant fibrous stroma.

There was a report that scirrhous HCC included two types: 1) one with dense fibrosis as in cholangiocarcinoma; and 2) one with a central scar with lamellar fibrosis as in fibrolamellar HCC. The second type might be the same as scalloped HCC in the present case.

On histology, there is a central scar consisting of coarse fibrosis and lamellar or dense fibrous bands dividing the tumors into small parts in various sizes. These tumor cells do not show oncocyte-like features such as in fibrolamellar HCC. Fibrous bands are connected from the central scar to the peripheral margin of the tumor, so scalloped HCC has a lobulated tumor margin without distinct capsule formation.

Scirrhous HCC with a central scar and scalloped margin tends to appear in patients with non-cirrhotic liver and a lower serum level of AFP compared to usual HCC; therefore, it is difficult to differentiate from cholangiocarcinoma, fibrolamellar HCC or FNH in some cases.

The recurrence rates of scalloped HCC are not different from those of simple nodular HCC. However, the time of recurrence is later, and the 5- and 10-year survival rates are better in patients with scalloped HCC than in patients with simple nodular HCC.

### References

1. Lee JH, Choi MS, Gwak GY, et al. Clinicopathologic characteristics and long-term prognosis of scirrhous hepatocellular carcinoma. Dig. Dis. Sci. 2012;57:1698-1707
2. Kim SH, Lim HK, Lee WJ, et al. Scirrhous hepatocellular carcinoma: comparison with usual hepatocellular carcinoma based on CT-pathologic features and long-term results after curative resection. Eur. J. Radiol. 2009;69:123-130
3. Leon TY, Kim SH, Lee WJ, et al. The value of gadobenate dimeglumine-enhanced hepatobiliary-phase MR imaging for the differentiation of scirrhous hepatocellular carcinoma and cholangiocarcinoma with or without hepatocellular carcinoma. Abdom Imaging 2010;35:337-345
4. Yamamoto M, Ariizumi S, Yoshitoshi K, et al. Hepatocellular carcinoma with a central scar and a scalloped tumor margin resembling focal nodular hyperplasia in macroscopic appearance. J. Surg. Oncol. 2006;94:587-591

# Case 5: Genitourinary


| | |
|---|---|
| Discusser | Hak Jong Lee |
| Country | Republic of Korea |
| Current Affiliation | Seoul National University Bundang Hospital |


| | |
|---|---|
| Age/Gender | 43/F |
| Chief complaint | Abdominal pain (1 month ago) |

A


B

C

D

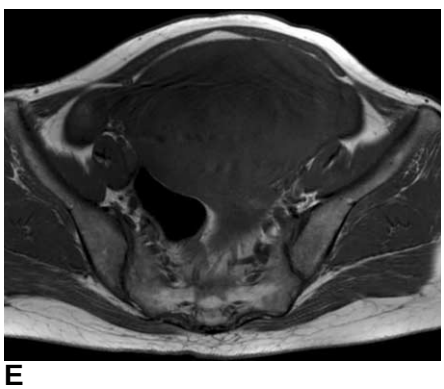

E

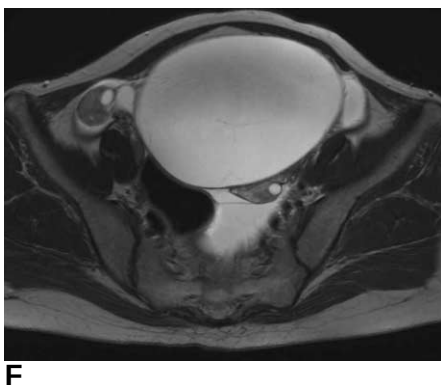

F

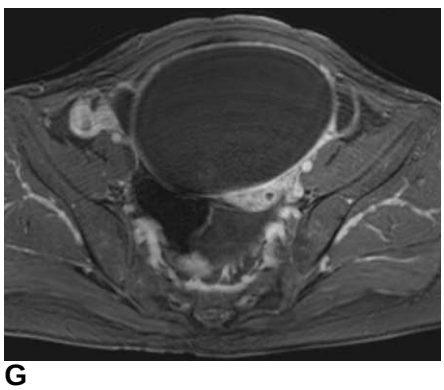

G

## Case 5

### History

A 43-year-old female presented with lower abdominal pain for one month.

### Findings

Outside US images depicted multiseptated cystic lesions combined with a large unilocular cystic lesion in the pelvic cavity. On CT images, there were several multiseptated and unilocular cystic masses with or without ascites in the lower abdomen and pelvis. Both ovarian tissues were located within those cystic lesions. No enhancing solid portion within the cystic mass was seen. MR images also demonstrated similar findings with those of CT images. On both T1- and T2WI showed multiseptated cystic masses around the uterus, while the uterus, fallopian tubes, and both ovaries look normal in shape except several small intramural leiomyomas in the uterus. In addition, CT images showed two lobulated cystic lesions with peripheral rim enhancement in the portocaval space and perihepatic space, respectively. A focal scalloping without the parenchymal invasion was noted at the hepatic parenchyma adjacent to the perihepatic lesion.

### Differential Diagnosis

Tuberculous peritonitis
Primary ovarian epithelial tumor with peritoneal seeding
Peritoneal seeding with unknown primary

### Diagnosis: *Tuberculous peritonitis*

### Discussion

Genital tract involvement was detected in 1.3% of female patients with tuberculosis, and the affected sites were the endometrium (72%), salpinx (34%), ovary (13%), and cervix (2%). Tubo-ovarian involvement is usually caused by hematogenous or lymphatic spread and occasionally by peritoneal dissemination. It can mimic ovarian cancer by both radiologic and clinical findings; the symptoms are usually vague, serum CA-125 levels are usually elevated, and the radiologic findings closely resemble those of ovarian cancer with peritoneal seeding. Therefore, the definite diagnosis is usually made postoperatively.

When overt tubo-ovarian abscesses (TOA) are formed by tuberculosis, complex adnexal masses with a large amount of ascites may be demonstrated on US, resembling ovarian malignancies with peritoneal seeding. When ovaries and salpinges are affected by peritoneal tuberculosis, tubo-ovarian lesions are usually minimal or even inconspicuous on CT, whereas the findings of tuberculous peritonitis frequently mimic those of peritoneal carcinomatosis. MRI is more helpful in revealing tubo-ovarian lesions and may demonstrate thickened salpinges or nodularities along tubo-ovarian surfaces. However, these findings are also nonspecific and differentiation from peritoneal seeding or primary ovarian malignancy such as serous surface papillary carcinomas is difficult. Some helpful findings suggestive of tuberculous peritonitis are smoother peritoneal thickening at CT and a more regular pattern of small nodularities along the peritoneum on MRI. Calcifications may be found in adnexal masses on CT and suggest tuberculosis but are not frequently observed, especially in active inflammation. Lymph node enlargement is common, and necrotic lymph nodes suggesting tuberculous lymphadenitis may be found.

On MRI, the walls of tuberculous TOAs are often irregular and show hypointensity on T2WI. Compared with usual TOAs, in which the wall thickening is usually uniform, tuberculous TOA may show a serrated or nodular inner wall. Dense adhesion with the uterus or other adjacent organs is common and reflects a late fibrotic process of this infection.

### References

1. Kim SH, Yang DM, Kim KA. Unusual causes of tubo-ovarian abscess: CT and MR imaging findings. Radiographics 2004;24:1575-1589
2. Crowley JJ, Ramji FG, Amundson GM. Genital tract tuberculosis with peritoneal involvement: MR appearance. Abdom Imaging 1997;22:445-447
3. Rodriguez E, Pombo F. Peritoneal tuberculosis versus peritoneal carcinomatosis: distinction based on CT findings. J Comput Assist Tomogr 1996;20:269-272
4. Barutcu O, Erel HE, Saygili E, Yildirim T, Torun D. Abdominopelvic tuberculosis simulating disseminated ovarian carcinoma with elevated CA-125 level: report of two cases. Abdom Imaging 2002;27:465-470

# Case 6: Pediatric


| | |
|---|---|
| **Discusser** | Choon-Sik Yoon |
| **Country** | Republic of Korea |
| **Current Affiliation** | Gangnam Severance Hospital |


| | |
|---|---|
| **Age/Gender** | 16/F |
| **Chief complaint** | Multiple bony masses, P/Hx Right humerus fracture (10 months ago) |

**A**

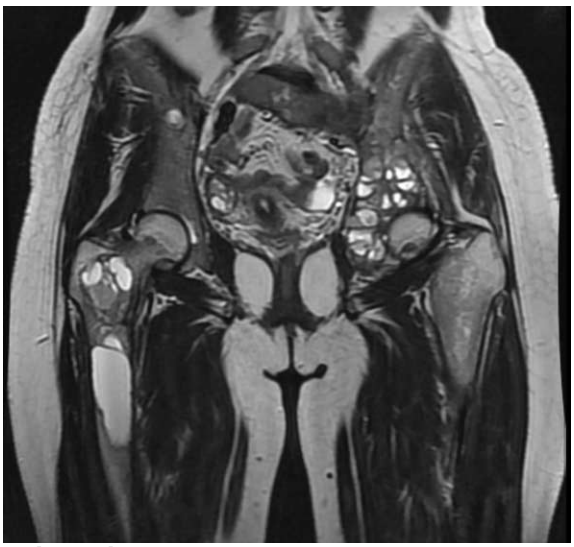

**B (T2WI)**

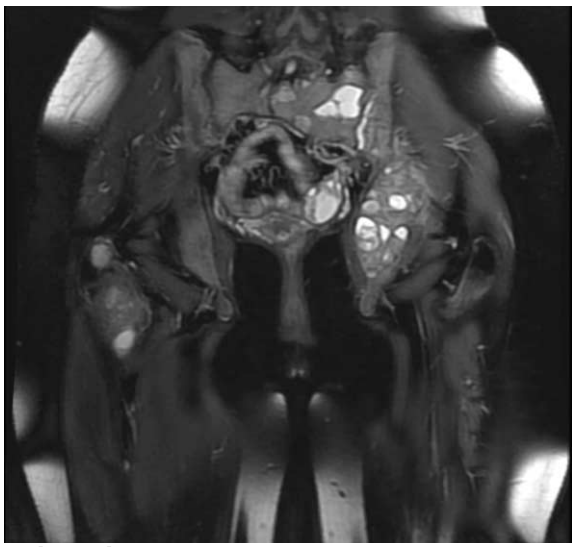

**C (STIR)**

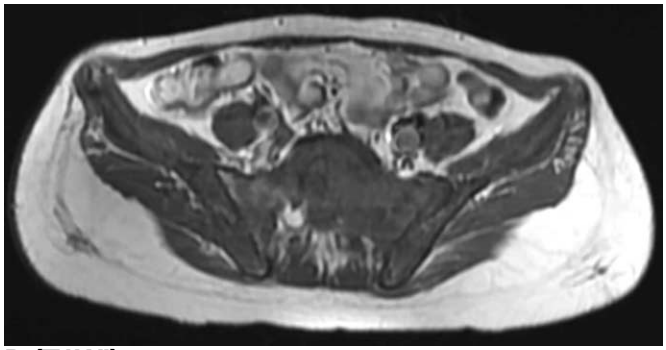

**D (T1WI)**

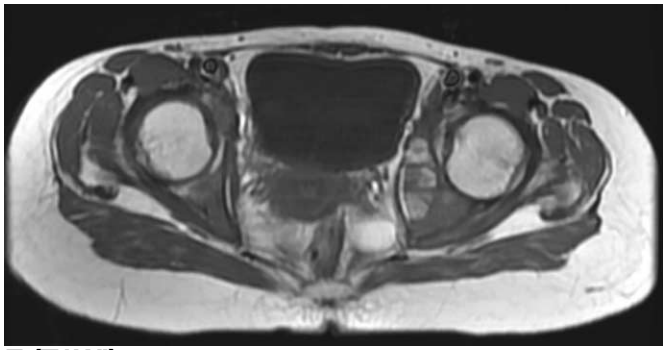

**E (T1WI)**

**F**

**G**

**H**

## Case 6

### History

A 16-year-old girl presented with progressive left hip pain for 8 months. She had an episode of right humerus fracture 10 months age without history of trauma. Laboratory exam. showed an elevated serum calcium level of 11.9 mEq/l (normal 4.2–5.2 mEq/l) and serum intact parathyroid hormone (iPTH) level of 2091 pg/ml (normal 15–50 pg/ml).

### Findings

Anteroposterior radiograph of the pelvis, lateral radiograph of the femur and anteroposterior radiograph show multifocal expansile osteolytic lesions involving bilateral pelvic bones and proximal femurs.

On MRI, the lesions have solid and cystic components. The solid components show hypointensity on T1WI and heterogeneous intermediate to hypointensity on T2WI. Multifocal cystic areas show fluid-fluid levels on T2WI. Neither reactive edema of adjacent bone marrow nor soft tissue is seen.

10 months age when the patient had an episode of right humerus fracture, radiograph showed an expansile osteolytic lesion with pathologic fracture. Note that several small osteolytic lesions and subperiosteal bone resorption at the right humeral head and scapula. On T1WI, the lesion revealed a septated cystic lesion with fluid-fluid level. After contrast material injection, the septa of the cystic lesion and adjacent muscles were enhanced.

Whole body bone 99mTc-MDP scintigraphy showed multiple foci of increased uptake on the skull, maxilla, mandible, both humerus, right ulna, both ribs, vertebrae, pelvic bones, femurs, and tibias.

A solitary adenoma of the left lower parathyroid gland was identified by 99mTc-methoxyisobutylisonitrile (MIBI) scintigraphy and US scan.

### Differential Diagnosis

Langerhans' cell histiocytosis
Giant cell tumors with ABC change
Fibrous dysplasia with ABC formation
Osteolytic metastases
Bone cysts

**Diagnosis:** *Brown tumor with primary hyperparathyroidism*

### Discussion

Brown tumors are nonneoplastic, osteolytic lesion of the bone caused by primary or secondary hyperparathyroidism. It can occur as solitary or multiple lesions in any bone, but commonly affects the pelvis, ribs, femur, other long bones, facial bones, metacarpals, phalanges, clavicle, spine, and rarely the sphenoid sinus.

The name of brown tumor arises from its grossly brownish color on biopsy due to the rich vascularity, hemorrhage, and hemosiderin deposition. Histopathologically it is characterized by hypervascular fibroblastic stroma, foci of hemorrhage, and accumulation of osteoclastic multinucleated giant cells.

Radiographically, brown tumors are seen as expansile lytic lesions. The cortex may be thinned or fractured. Other imaging findings of hyperparathyroidism can be associated with brown tumor including osteopenia, subperiosteal bone resoption, and pathologic fracture. On MRI, they are single or multifocal lesions of a cystic nature mixed with or without solid lesions. The solid portions are iso to hypointense on the T1- and T2WI and the cystic portions are hyperintense on the T2WI. The solid portions and the septa of the cystic portions are well enhanced. Cortical destruction and soft-tissue extension can be seen.

### References

1. Hong WS, Sung MS, Chun KA, Kim JY, Park SW, Lee KH, et al. Emphasis on the MR imaging findings of brown tumor: a report of five cases. Skeletal Radiol 2011;40:205-13
2. Takeshita T, Takeshita K, Abe S, Takami H, Imamura T, Furui S. Brown tumor with fluid-fluid levels in a patient with primary hyperparathyroidism: radiological findings. Radiat Med 2006;24: 631-634
3. Miyakoshi M, Kamoi K, Takano T, Nishihara M, Kawashima T, Sudo N, et al. Multiple brown tumors in primary hyperparathyroidism caused by an adenoma mimicking metastatic bone disease with false positive results on computed tomography and Tc-99m sestamibi imaging: MR findings. Endocr J 2007; 54:205-210

# *Case 7: Neuro*



| | |
|---|---|
| **Discusser** | Dae Seob Choi |
| **Country** | Republic of Korea |
| **Current Affiliation** | Gyeongsang National University Hospital |



| | |
|---|---|
| **Age/Gender** | 25/F |
| **Chief complaint** | Left-side weakness and paresthesia |

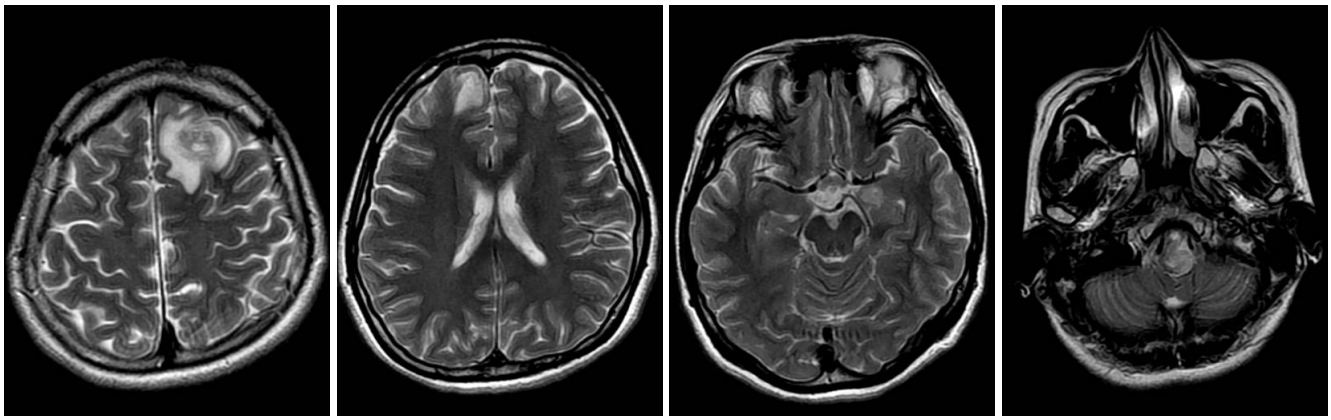


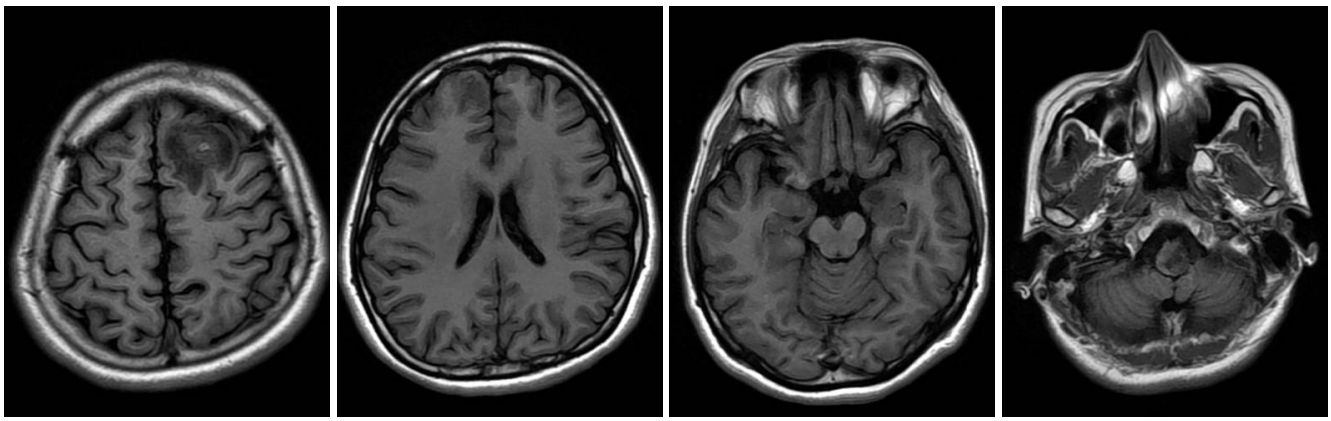


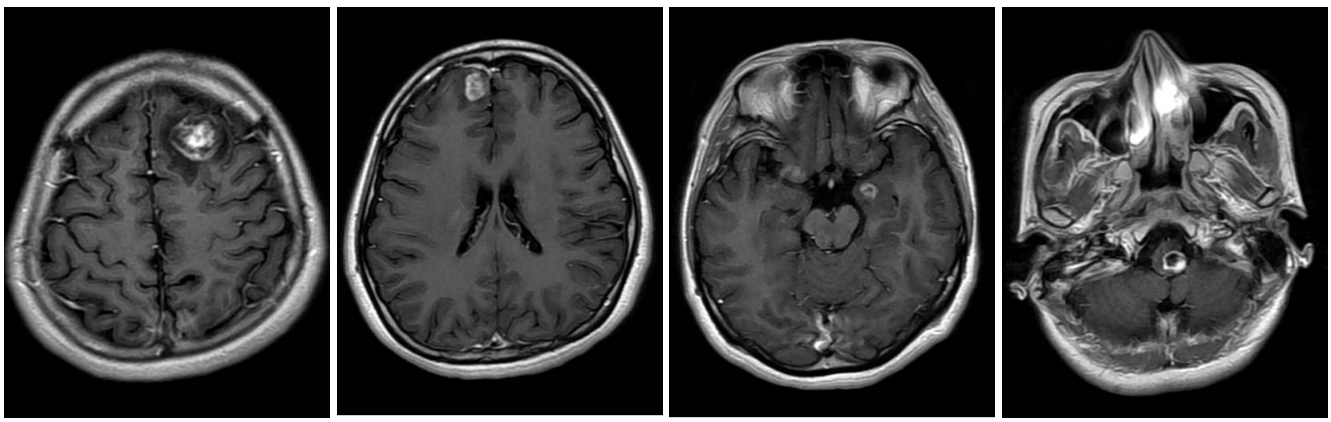

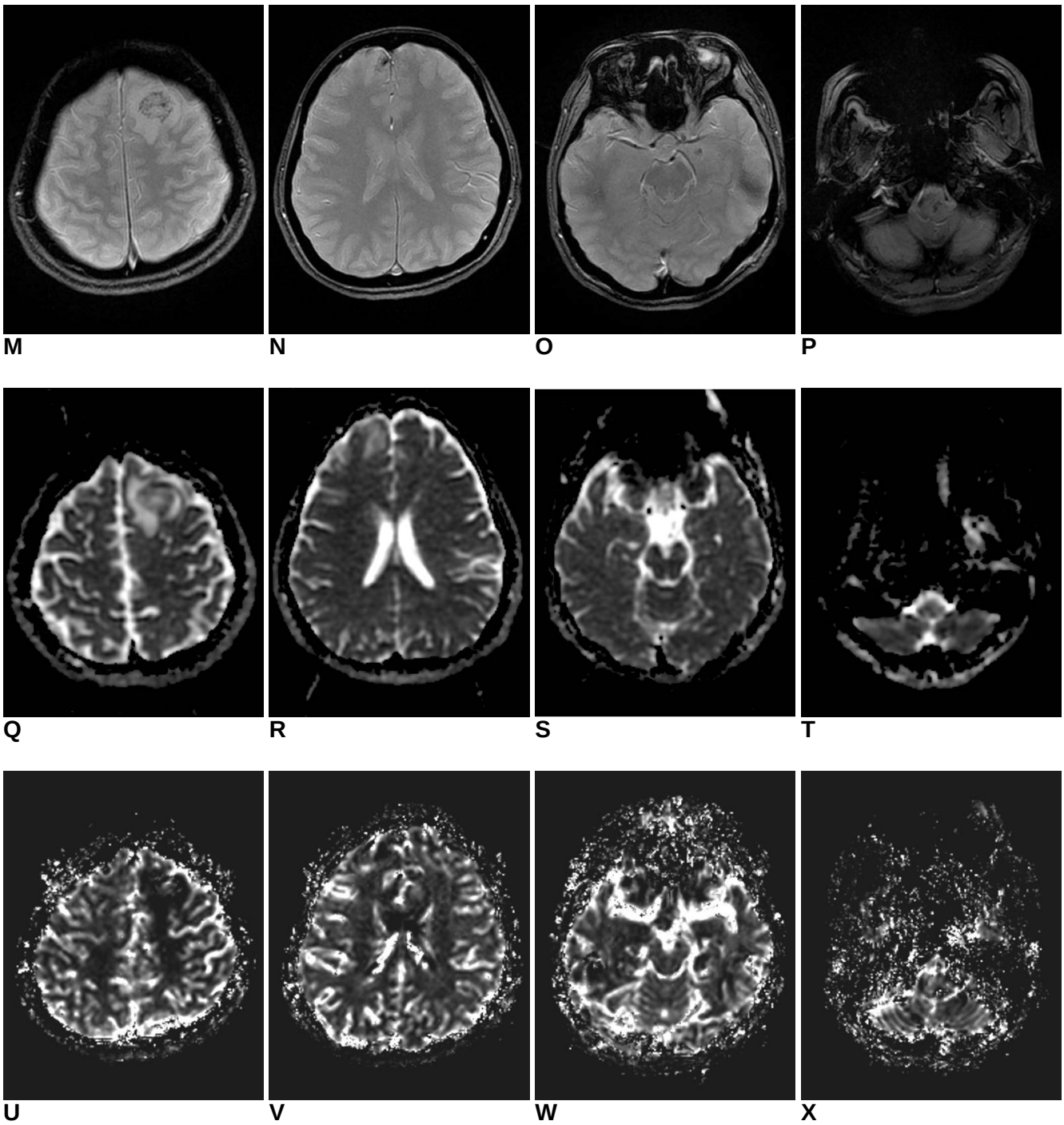
M
N
O
P
Q
R
S
T
U
V
W
X

## Case 7

### History

A 25-year-old female presented with left side weakness and hyperesthesia in her body and face for a week with nausea, vomiting, dizziness and fatigue.

### Findings

Multiple cortical or subcortical lesions are present in bilateral frontal lobe, left mediobasal temporal lobe and left medulla oblongata. On T2WI, there is a peri-lesional edema. On T1WI, focal hyperintenstiy, which is suspected as a hemorrhagic component, is present in the largest lesion in the left frontal lobe. Gradient echo images confirm the existence of internal hemorrhagic components in all lesions. These lesions show thick and irregular peripheral rim enhancement on contrast enhancement study and non-enhancing foci are considered to be a necrotic component.

On DWI, the largest lesion in the left frontal lobe shows diffusion restrictive component, which is considered to be cystic areas consistent with necrosis. Perfusion weighted images reveal that a lack of rCBV increment in all lesions.

### Differential Diagnosis

Primary CNS lymphoma
Metastases

### Diagnosis: *Primary CNS T-cell lymphoma*

### Discussion

In general, CNS T-cell lymphoma (T-PCNSL) is more prevalent in Eastern countries, of which the incidence was 16.7% in Korea.

In Eastern countries, T-PCNSL is more likely to be located in either the supratentorial or subcortical areas.

Necrosis and hemorrhage are more often noted in the PCNSL of immunocompromised patients and are scarce in immunocompetent patients. And T-PCNSL showed necrosis more frequently than CNS B-cell lymphoma (B-PCNSL). Some T-PCNSLs showed high and low signal intensity on the DWI and ADC map, respectively, as well as finding of cystic areas consistent with necrosis, which raises the possibility of an abscess.

Homogeneous enhancement has generally been considered to be a characteristic finding of PCNSL, but the T-PCNSL showed rim enhancement or heterogeneous enhancement, which is dissimilar to the enhancement pattern of B-PCNSL. T-PCNSL mostly consists of small-sized cells which are interspersed without forming a solid mass, while B-PCNSL is commonly composed of large cells that crowd together to form monomorphous sheets. These different pathologic manifestations may give rise to their distinct enhancement patterns: heterogeneous enhancement in T-PCNSL and homogeneous enhancement in B-PCNSL.

On perfusion-weighted imaging, it was reported that neo-vascularization is not identified in PCNSL, in contrast to anaplastic gliomas. Thus, PWI can be used to differentiate cerebral lymphomas from anaplastic gliomas. Nevertheless, further studies should be con-ducted to determine the usefulness of PWI in differentiating T-PCNSL from high-grade gliomas.

### References

1. Choi JS, Nam DH, Ko YH, Seo JW, Choi YL, Suh YL, et al. Primary central nervous system lymphoma in Korea: comparison of B- and T-cell lymphomas. Am J Surg Pathol 2003;27:919-28
2. Coulon A, Lafitte F, Hoang-Xuan K, Martin-Duverneuil N, Mokhtari K, Blustajn J, et al. Radiographic findings in 37 cases of primary CNS lymphoma in immunocompetent patients. Eur Radiol 2002;12:329-40
3. Kim EY, Kim SS. Magnetic resonance findings of primary central nervous system T-cell lymphoma in immunocompetent patients. Acta Radiol 2005;46:187-192
4. Kleihues P, Burger PC, Scheithauer BW. Histological typing of tumours of the centeral nervous system. Berlin: Springer Verlag; 1999
5. Hartmann M, Heiland S, Harting I, Tronnier VM, Sommer C, Ludwig R, et al. Distinguishing of primary cerebral lymphoma from high-grade glioma with perfusion-weighted magnetic resonance imaging. Neurosci Lett 2003;338:119-22

# Case 8: Chest


| | |
|---|---|
| **Discusser** | Hwan Seok Yong |
| **Country** | Republic of Korea |
| **Current Affiliation** | Korea University Guro Hospital |


| | |
|---|---|
| **Age/Gender** | 60/M |
| **Chief complaint** | Abnormal chest radiograph |

A

B

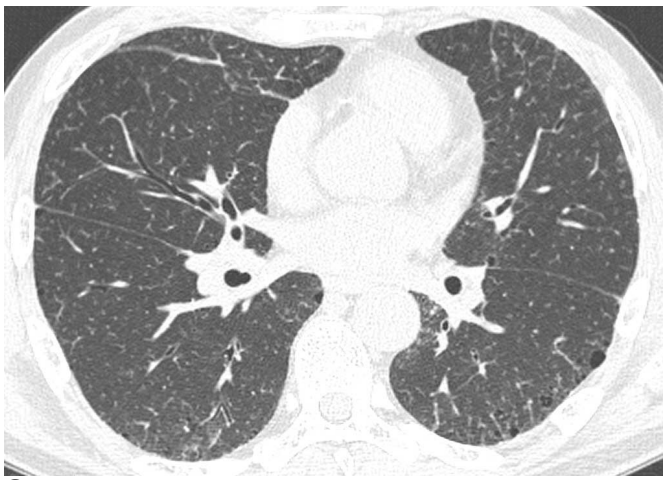

C

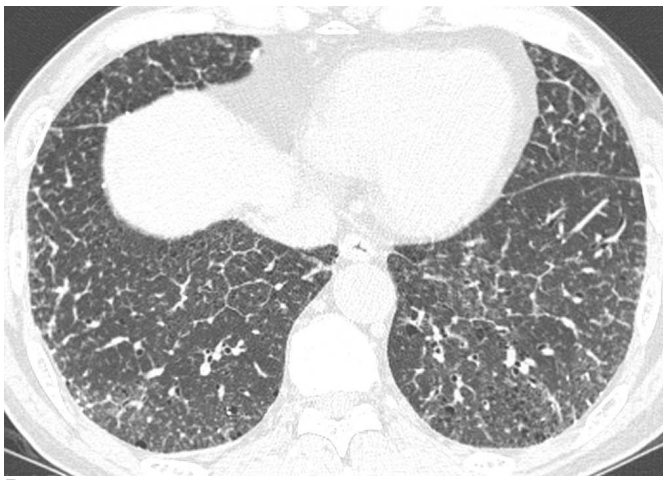

D

## Case 8

### History

A 60-year-old man presented with an abnormal chest radiographic finding.

### Findings

Plain chest radiograph showed diffusely increased interstitial markings in both lower lungs. Chest HRCT scan showed diffuse interlobular septal thickening and diffuse centrilobular micronodules plus subpleural nodules (so called, perilymphatic nodules), which were more prominent in the lower lung zones. Also, multiple punctate calcifications are noted in the micronodules.

### Differential Diagnosis

Diseases that can manifest perilymphatic nodules among diffuse micronodular lung diseases include:

- Sarcoidosis
- Pneumoconiosis
- Hematolymphangitic carcinomatosis
- Amyloidosis.

**Diagnosis:** *Amyloidosis, primary, a diffuse interstitial form, involving gastrointestinal tracts and lungs, in a patient with multiple myeloma*

- *Stomach biopsy performed due to hematemesis symptom:*
- *Amorphous material deposition in lamina propria; c/w amyloidosis*
- *Bone marrow biopsy:*
- *Plasma cell myeloma*

### Discussion

Amyloidosis is a constellation of disease entities characterized by the abnormal extracellular deposition and accumulation of fibrillar protein and protein derivatives. Primary amyloidosis is associated with plasma cell dyscrasia, such as plasma cell myeloma or MGUS, and secondary amyloidosis can be seen in chronic inflammatory conditions or tissue-destructive processes such as rheumatoid arthritis or inflammatory bowel diseases. It can manifest either a systemic (80–90%) or a localized (10–20%) form.

Primary amyloidosis occurs in 5–12 persons/million per year, and 20% of them progress to multiple myeloma. It can involve kidneys, heart, gastrointestinal tracts, peripheral nerves, liver, and spleen. The respiratory system is also involved in 50%. The treatment of amyloidosis includes chemotherapy, ASCT, organ transplantation, and surgery.

Pulmonary amyloidosis manifests one of three forms: tracheobronchial, nodular parenchymal, and diffuse interstitial form. The tracheobronchial pattern is most common, and manifests as focal or diffuse thickening with luminal narrowing of the tracheobronchial wall.

The nodular parenchymal pattern shows a solitary or multiple well-defined nodules (amyloidoma, 0.5–5 cm), which are located most commonly in the lower lobes, showing calcification in 20%-50%. The diffuse interstitial pattern is least common with a poor prognosis, usually seen in multiple myeloma. The HRCT shows widespread interlobular septal thickening, irregular lines, and diffuse perilymphatic micronodules with some punctate calcifications, which are more prominent in the lower lungs.

### References

1. Pickford HA, Swensen SJ, Utz JP. Thoracic cross-sectional imaging of amyloidosis. AJR Am J Roentgenol 1997;168(2):351-355
2. Georgiades CS, Neyman EG, Barish MA, Fishman EK. Amyloidosis: review and CT manifestations. Radiographics 2004;24(2):405-416
3. Urban BA, Fishman EK, Goldman SM, et al. CT evaluation of amyloidosis: spectrum of disease. Radiographics 1993;13(6):1295-1308

# Case 9: Abdomen


| | |
|---|---|
| **Discusser** | Hun Kyu Ryeom |
| **Country** | Republic of Korea |
| **Current Affiliation** | Kyungpook National University Hospital |


| | |
|---|---|
| **Age/Gender** | 68/F |
| **Chief complaint** | Known EGC IIa+IIc in antrum on gastroscopy |

**A (EGD)**

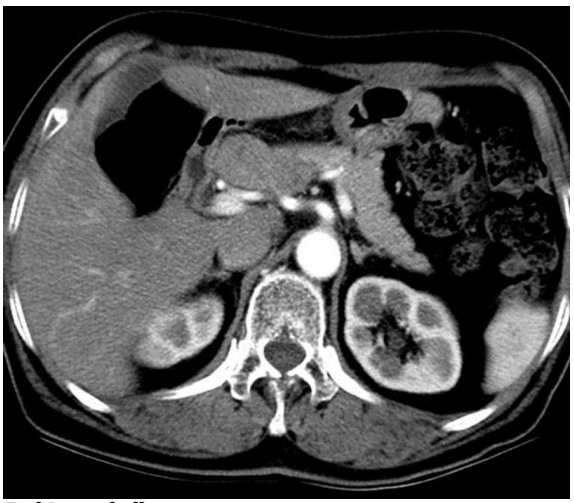

**B (Arterial)**

**C (Portal)**

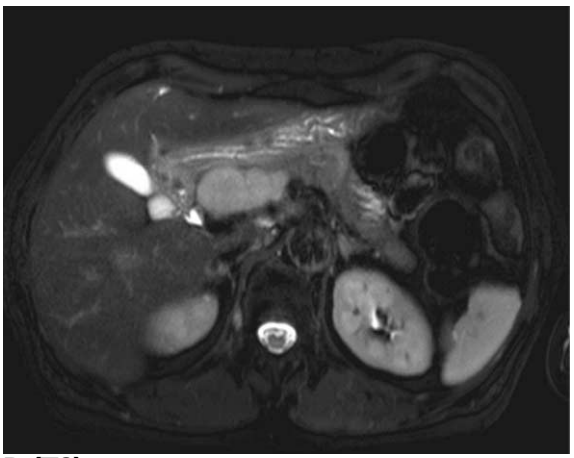

**D (T2)**

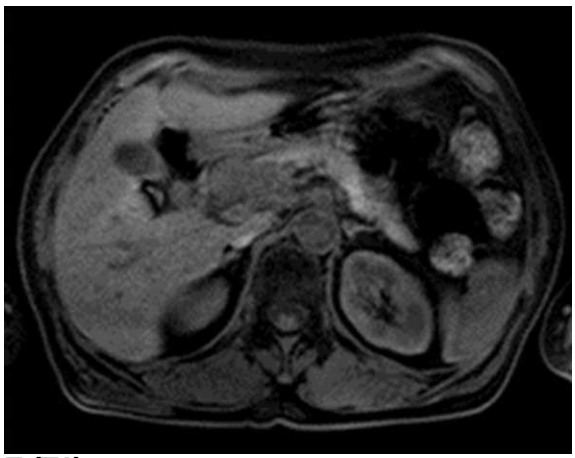

**E (T1)**

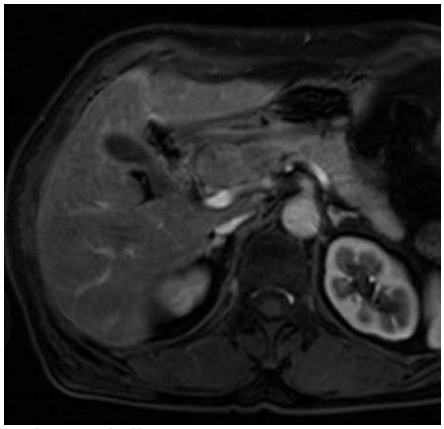

**F (Arterial)**

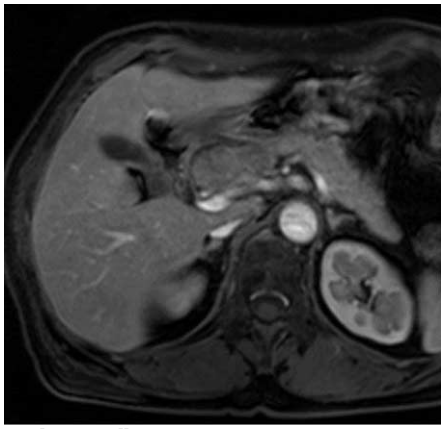

**G (Portal)**

**H (Delay)**

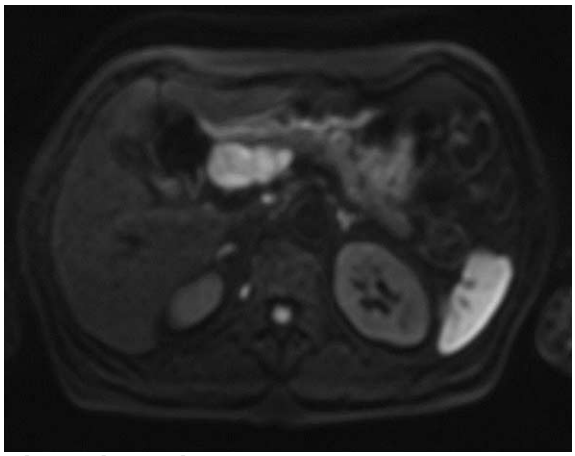

**I (DWI, b=800)**

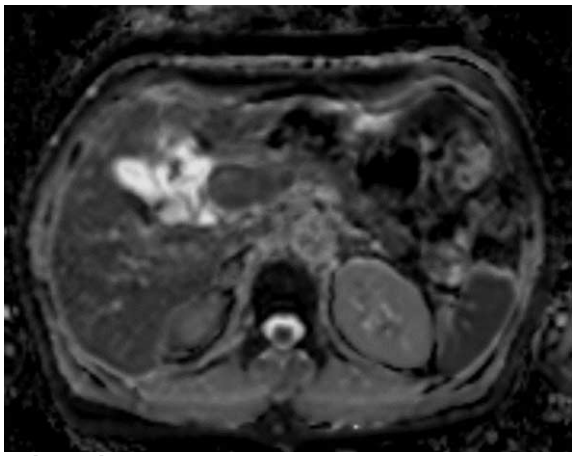

**J (ADC)**

## Case 9

### History

A 68-year-old female diagnosed as early gastric cancer (EGC) type IIa+IIc in the antrum on endoscopy.

### Findings

Preoperative contrast-enhanced CT scan revealed no abnormality in the stomach and no evidence of distant metastasis. However, a 3.2 cm mass was detected around common hepatic artery which abutted the pancreas. It showed well-defined margin and relatively homogenous enhancement. Its degree of enhancement was less than adjacent pancreas parenchyma.

On MRI, the mass showed hypointensity on T1WI, hyperintensity on T2WI, and less contrast enhancement compared with the pancreas on dynamic images. DWI revealed diffusion restriction. It was impossible to discriminate between intra- and extra pancreatic location of the mass even on MRI. Finally, US was performed to localize the mass. It showed a sliding motion against the pancreas during the patient's respiration.

### Differential Diagnosis

Metastatic lymph node from EGC

Exophytic pancreatic tumor

- Neuroendocrine tumor
- Solid pseudopapillary tumor

### Diagnosis: *Metastatic lymph node from EGC*

- *Subtotal gastrectomy and regional lymph node dissection: single metastatic lymph node in the area of common hepatic artery (T1bN1).*

### Discussion

The incidence of lymph node metastasis has been reported to range from 2.6 to 4.8% in EGC patients. While the prognosis for surgically treated EGC is excellent, with 5-year survival greater than 90%, patients with lymph node metastasis have lower survival rates than those without metastasis. The recurrence rate is higher in patients with lymph node metastasis than in patients without that (7–20% vs. 0.6–0.7%).

Unlike the stationary imaging modality such as CT and MR, ultrasonography gives us the real time monitoring of targeted lesion with some intervention such as respiratory movement. Based on the fact that intraperitoneal and retroperitoneal organs move differently during respiration, we can observe the same phenomenon demonstrated between extra- and intra-pancreatic lesions, called sonographic sliding sign.

In this case, sonographic sliding sign is a valuable clue in making a correct diagnosis differentiating between a intra- and extra-pancreatic localization when CT and MR has been inconclusive. When we wonder if the origin of lesion is between intra and retro-peritoneal location, it could lead to limit the differential diagnosis.

### References

1. Park CH, Song KY, Kim SN. Treatment results for gastric cancer surgery: 12 years' experience at a single institute in Korea. Eur J Surg Oncol 2008;34:36-41
2. Haruta H, Hosoya Y, Sakuma K, Shibusawa H, Satoh K, Yamamoto H, Tanaka A, et al. Clinicopathological study of lymph-node metastasis in 1,389 patients with early gastric cancer: assessment of indications for endoscopic resection. J Dig Dis 2008;9:213-218
3. Nam MJ, Oh SJ, Oh CA, Kim DH, Bae YS, Choi MG, Noh JH, et al. Frequency and predictive factors of lymph node metastasis in mucosal cancer. J Gastric Cancer 2010;10: 162-167
4. Lim HK, Kim S, Lim JH, Kim SH, Lee WJ, Chun H, Cho JW, et al. Assessment of pancreatic invasion in patients with advanced gastric carcinoma: usefulness of the sliding sign on sonograms. AJR Am J Roentgenol 1999;172:615-618
5. Lim JH, Ko YT, Lee DH. Sonographic sliding sign in localization of right upper quadrant mass. JUM 1990;9:455-459

# *Case 10: Genitourinary*


| | |
|---|---|
| **Discusser** | Hak Jong Lee |
| **Country** | Republic of Korea |
| **Current Affiliation** | Seoul National University Bundang Hospital |


| | |
|---|---|
| **Age/Gender** | 49/M |
| **Chief complaint** | Right scrotal pain (2 months ago) |

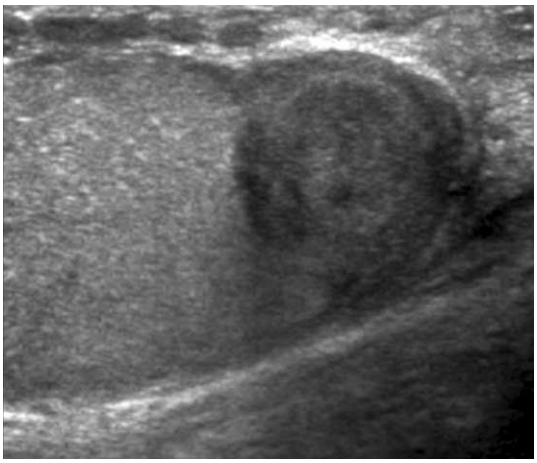

**A**

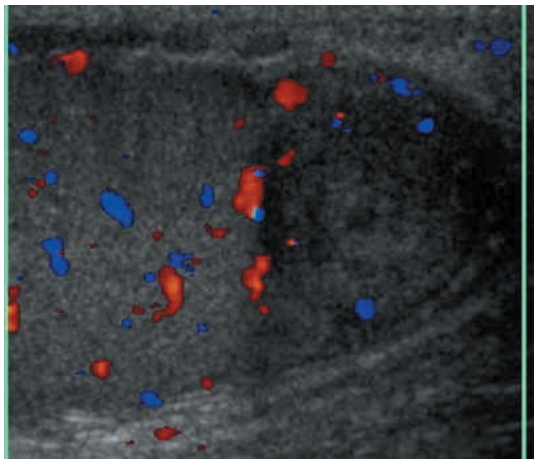

**B**

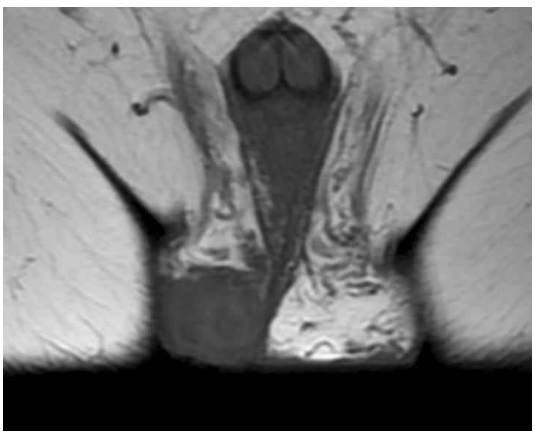

**C**

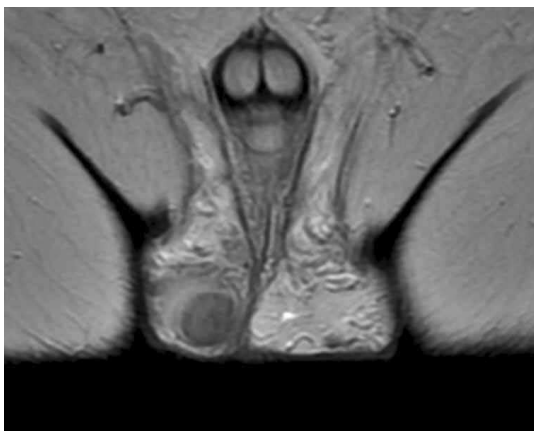

**D**

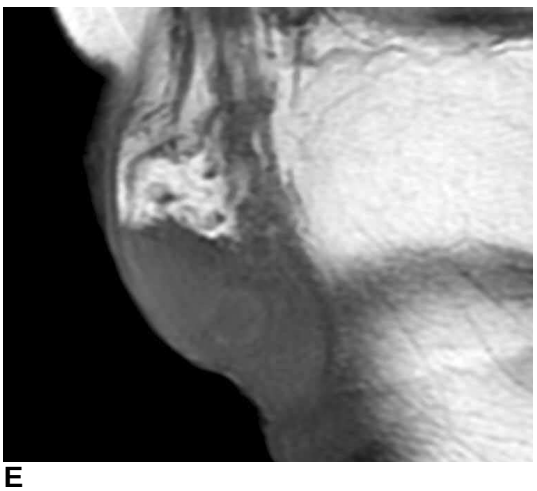

**E**

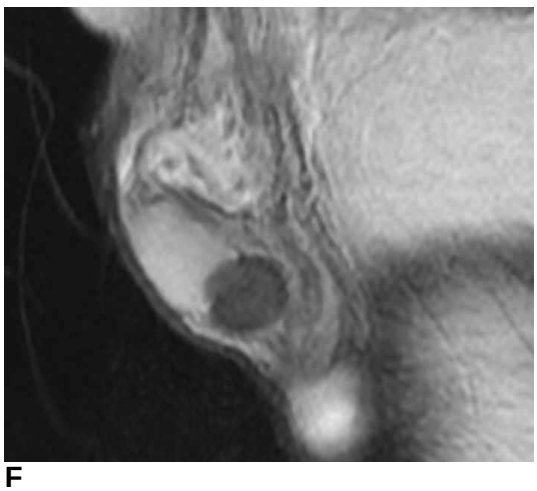

**F**

## Case 10

### History

A 49-year-old male presented with right scrotal pain for 2 months. Serum AFP and HCG levels were within normal range.

### Findings

The US images depicted a 1.5 cm mass showing heterogeneous echotexture in the right testis. On color doppler images, the mass showed minimal vascularity. The origin of the lesion was not clearly determined because it abuts both the testis and epididymal tail. MRI demonstrates an exophytic mass in the right testis showing isointensity on T1WI and heterogeneous hypointensity relative to the testicular parenchyma on T2WI. The epididymis looks separated from the mass, and the mass seems to be a paratesticular lesion. Contrast-enhanced images were not obtained.

### Differential Diagnosis

Epidermoid cyst
Non-seminomatous germ cell tumor
Abscess
Benign tumor originating from tunica albuginea.

**Diagnosis:** *Adenomatoid tumor originating from tunica albuginea.*

### Discussion

Adenomatoid tumor is the most common paratesticular neoplasms and account for approximately 30% of all paratesticular neoplasms. It occurs in men with a wide range of ages, with the majority in patients aged 20–50 years. Patients usually present with a painless scrotal mass. The tumors are smooth, round, well-defined and vary in size from 0.4–5.0 cm. Although more frequent in the tail, adenomatoid tumor may occur anywhere in the epididymis and have also been reported in the spermatic cord, paratesticular tissue and tunica albuginea, where they can grow intratesticularly. Thus these lesions can extend into the testis from a paratesticular location, and it may be necessary to obtain an MRI after an initial US to prove their extratesticular origin.

The histologic nature of adenomatoid tumors has been a source of controversy, with most investigators suggesting a mesothelial origin. In female subjects, adenomatoid tumors are commonly found in the uterus and fallopian tubes. Because of the benign nature of this tumor, the treatment of choice is local excision.

On US, they appear nonspecific and variable, although the majority appears isoechoic and homogeneous. When the epididymis is involved, it is easily identified as extratesticular. When the lamina parietalis of the tunica vaginalis is involved, they cannot be differentiated from peripheral testicular tumors in the absence of fluid collection.

MRI demonstrates hypointensity relative to the testicular parenchyma on T2WI. MRI can aid in determining the paratesticular origin of the lesion. After contrast material injection, slow or decreased enhancement relative to the normal testis may be demonstrated and also suggest a benign condition.

### References

1. Park SB, Lee WC, Kim JK, et al. Imaging features of benign solid testicular and paratesticular lesions. Eur Radiol 2011;21:2226-2234
2. Akbar SA, Sayyed TA, Jafri SZH, Hasteh F, Neill JSA. Multimodality imaging of paratesticular neoplasms and their rare mimics. Radiographics 2003;23:1461-1476
3. Kim W, Rosen MA, Langer JE, Banner MP, Siegelman ES, Ramchandani P. US-MR Imaging correlation in pathologic conditions of the scrotum. Radiographics 2007;27